A Preliminary Report on the Tecomán, Mexico Earthquake of 22 January 2003 (M_w 7.4) and Its Effects

S. K. Singh[1,2], J. F. Pacheco[1], L. Alcántara[2], G. Reyes[3], M. Ordaz[2], A. Iglesias[1], S. M. Alcocer[2,4], C. Gutierrez[4], C. Valdés[1], V. Kostoglodov[1], C. Reyes[4], T. Mikumo[1], R. Quaas[2,4], and J. G. Anderson[5]

Contributions were made (in alphabetical order) by D. Almora[2], M. Ayala[2], G. Castro[2], J. L. Cruz[1], R. Duran[4], A. Echavarría[4], G. Espitía[4], J. Estrada[1], L. Flores[4], E. Guevara[4], C. Javier[6], C. Lopez[4], O. Lopez[4], M. Macías[2], E. Mena[6], M. Ortiz[7], M. A. Pacheco[4], C. Perez[2], J. A. Perez[1], M. Ramírez[3], M. Romo[2], A. Ruíz[2], H. Sandoval[2], M. Santoyo[1], M. Torres[2], E. Vázquez[2], R. Vazquéz[2], J. M. Velasco[2], and J. Ylizaliturri[2]

INTRODUCTION

The M_w 7.4 Tecomán earthquake occurred off the Pacific coast of the state of Colima, México on 22 January 2003 (Figure 1). It was felt very strongly in the city of Colima and the towns of Tecomán and Armería. The earthquake left 21 persons dead. About 15,000 houses suffered damage; roughly 3,000 of these experienced severe damage. The most significant damage was observed in adobe and unreinforced brick masonry houses. Very few cases of structural failure were recorded in engineered buildings. Ground motion in the lakebed zone of Mexico City, about 540 km from the epicentral zone, was strong enough to cause general panic in the population.

Over the last 100 years the coasts of Colima and the adjacent state of Jalisco have been struck by several large earthquakes: 3 June 1932, M_s 8.2; 18 June 1932, M_s 7.8; 22 June 1932, M_s 7.0; 30 January 1973, M_w 7.6; 9 October 1995, M_w 8.0. The earthquakes of 3 and 18 June 1932 devastated the states of Jalisco and Colima. The relatively small event of 22 June 1932 caused a large local tsunami on the coast of Cuyútlan, drowning many persons. The earthquake of 9 October 1995 caused extensive damage to Manzanillo and towns along the coast of Jalisco. These earthquakes had left a small gap between the rupture areas of the 1973 and 1995 events (Figure 1). This gap broke during the Tecomán earthquake. The purpose of this report is to present preliminary results on the earthquake and its effects.

1. Instituto de Geofísica, UNAM, México
2. Instituto de Ingeniería, UNAM, México
3. Red Sísmica de Colima, Universidad de Colima, Colima, México
4. Centro Nacional de Prevención de Desastres, México
5. Seismological Laboratory, Mackay School of Mines, University of Nevada, Reno
6. Comisión Federal de Electricidad, México, D.F., México
7. CICESE, Ensenada, México

TECTONICS AND RUPTURE AREAS OF EARTHQUAKES IN THE REGION

The tectonic setting of the region is outlined in Figure 1. In this region, the oceanic Rivera (RIVE) and Cocos (COCOS) Plates subduct below México, which forms part of the large North American (NOAM) Plate. The boundary between the RIVE and COCOS plates, as well as the relative convergence speed of the RIVE and NOAM plates, are still controversial. Bandy *et al.* (1995) suggest that the subducted RIVE-COCOS boundary lies directly beneath the Southern Colima Rift (SCR) and is parallel to it (Figure 1). The SCR extends from just south of the city of Colima to the Middle America Trench and is part of the Colima rift. According to Kostoglodov and Bandy (1995), the relative convergence speed between RIVE-NOAM and COCO-NOAM near the SCR is roughly equal and is about 5 cm/yr.

Figure 1 shows the aftershock zones of large/great earthquakes that have occurred in the region. The aftershock zones of the earthquakes of 3 and 18 June 1932 were estimated by Singh *et al.* (1985) from seismograms at Manzanillo and Guadalajara. The earthquake of 3 June (M_s 8.2; M_w 8.0) was the largest earthquake in Mexico during the 20th century. While this earthquake caused extensive damage in Jalisco, the intensities in the city of Colima were higher during the smaller 18 June event (Singh *et al.*, 1985).

The aftershock zone of the 1973 earthquake was reported by Reyes *et al.* (1979). A segment of about 50 km, which coincides with the Southern Colima Rift (Figure 1), was left unbroken between the aftershock areas of the 18 June 1932 and the 1973 events. The earthquake of 9 October 1995 initiated southeast of Manzanillo and propagated northwest for a length of about 110 km (Courboulex *et al.*, 1997; Pacheco *et al.*, 1997; Ortiz *et al.*, 1998). The large disparity between the estimated M_s and M_w values (7.3 versus

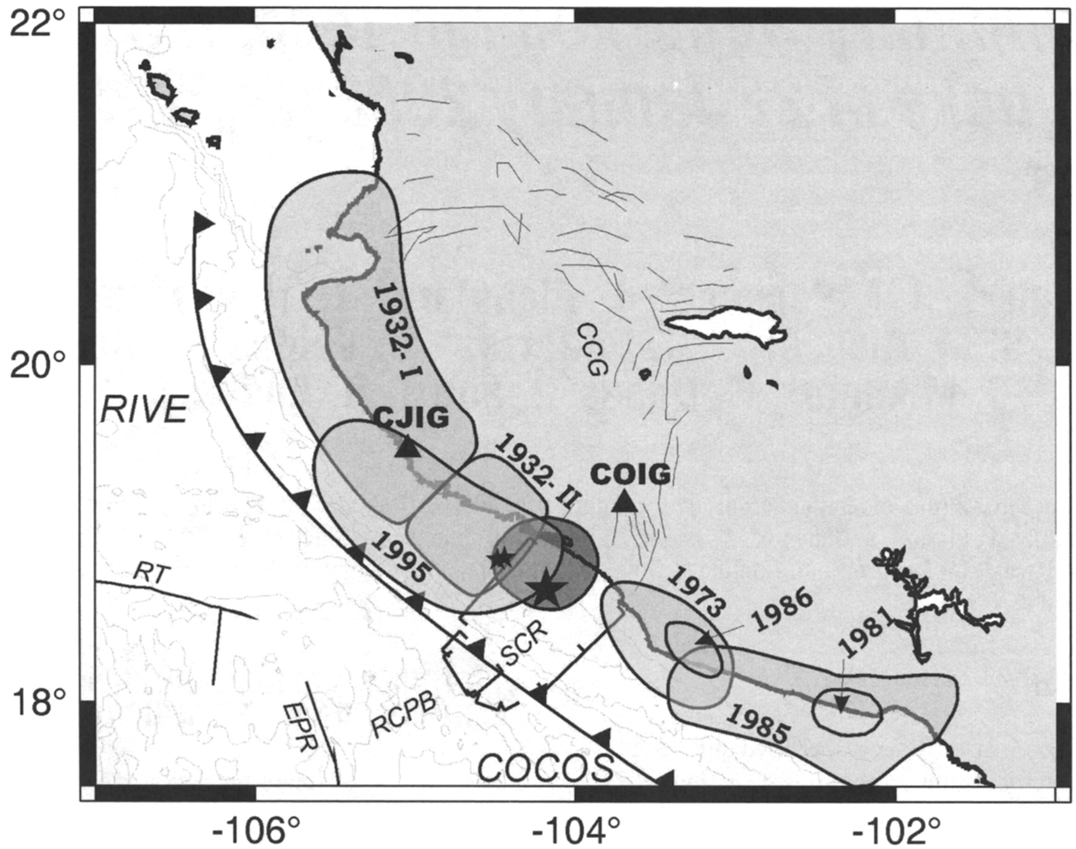

▲ **Figure 1.** Tectonic map of the region (modified from Bandy *et al.*, 1995, and Kostoglodov and Bandy, 1995). RT: Rivera Transform, EPR: East Pacific Rise, RCPB: Rivera Cocos Plate Boundary, SCR: Southern Colima Rift, CCG: Colima Central Graben. Ticked lines indicate areal extent of SCR rift. COIG and CJIG are BB stations. The contours outline aftershock areas of large/great earthquakes in the region. Large and small stars indicate the epicenters of the Tecomán mainshock and two of its largest aftershocks.

8.0, respectively) of the 1995 earthquake suggests a relatively slow, tsunamigenic earthquake (see also Shapiro *et al.*, 1998). Indeed, the coastal areas in the epicentral zone were hit by a tsunami (Ortiz *et al.*, 1996) that was unusually large for a Mexican subduction zone earthquake. Simultaneous inversion of permanent deformation data caused by the earthquake (as revealed by GPS measurements, Melbourne *et al.*, 1997) and regional seismograms reveals rupture extending till the trench (Bernal, 2000). No M_s–M_w disparity was found for the 1932 event. The aftershock zones of the events of 1995 and 3 June 1932 overlap only partly. This and the significant difference in the source parameters of the two events shows that they did not rupture the same segment of the plate interface (Pacheco *et al.*, 1997). It appears that the two events broke different widths of the plate interface, with the 1995 event rupturing more updip than the rupture of the 1932 event. This would also explain the much higher intensities and damage during the 1932 event.

The surface projection of the aftershocks of the 1995 earthquake covered part of the Southern Colima Rift (Figure 1). As we show below, the Tecomán rupture occurred below the rift with the northwest part of its aftershock zone overlapping with the southeast part of the aftershock zone of the 1995 event.

SOURCE PARAMETERS

The source parameters of the mainshock, as reported by RESCO (Red Sísmica de Colima), a local network operated by the University of Colima, SSN (Servicio Sismólogico Nacional), and some international sources are listed in Table 1.

Local and Regional Data

RESCO operates a conventional, telemetered, short-period network in the region. The mainshock seismograms of RESCO were clipped after the *P* wave. SSN maintains a broadband (BB) seismographic station, COIG, near the city of Colima (Figure 2). This station recorded accelerations for about 10 sec of the mainshock (essentially the *P*-wave group) before experiencing a failure that prevented further recording. It also recorded velocities for about 4 sec before going off scale. CIRES (Centro de Instrumentación y Registro Sísmico) maintains accelerographs in a thermal power plant in Manzanillo (epicentral distance ~55 km). Here the peak horizontal acceleration at a free-field, sandy-soil site reached 323 gals. The next closest site to produce an on-scale recording was Chamela (CJIG), a BB station of SSN (epicentral distance 137 km). The STS-2 seismometer at CJIG saturated but the accelerograms are available.

TABLE 1 Source Parameters of the 22 January 2003, Tecomán Earthquake									
Source	**Origin Time**	**Lat**	**Long**	**Depth (km)**	**Magnitude**	**M_0 (dyne-cm)**	**Strike**	**Dip**	**Rake**
RESCO[1]	02:06:33.8	18.625°	−104.125°	10	—	—	—	—	—
SSN[2]	02:06:34.6	18.60°	−104.22°	9.3	M_e 7.6[6]	—	—	—	—
NEIC/USGS[3]	02:06:34	18.84°	−103.82°	24.0	m_b 7.3, M_s 7.3	—	—	—	—
CMT[4]	02:06:47.3	18.77°	−103.89°	32.6	M_w 7.4	1.6×10^{27}	305°	17°	103°
Yagi[5]	—	18.625°	−104.125°	20.0	M_w 7.4	1.45×10^{27}	300°	20°	93°

1. RESCO: Red Sísmica de Colima, operated by University of Colima.
2. SSN: Servicio Sismológico Nacional, operated by the Instituto de Geofísica, UNAM.
3. Preliminary NEIC/USGS location.
4. Harvard CMT solution.
5. From inversion of teleseismic body waves. The epicenter reported by RESCO was used in the inversion.
6. M_e is based on radiated seismic energy estimated from seismograms at CUIG (Singh and Pacheco, 1994). It is tied to M_w.

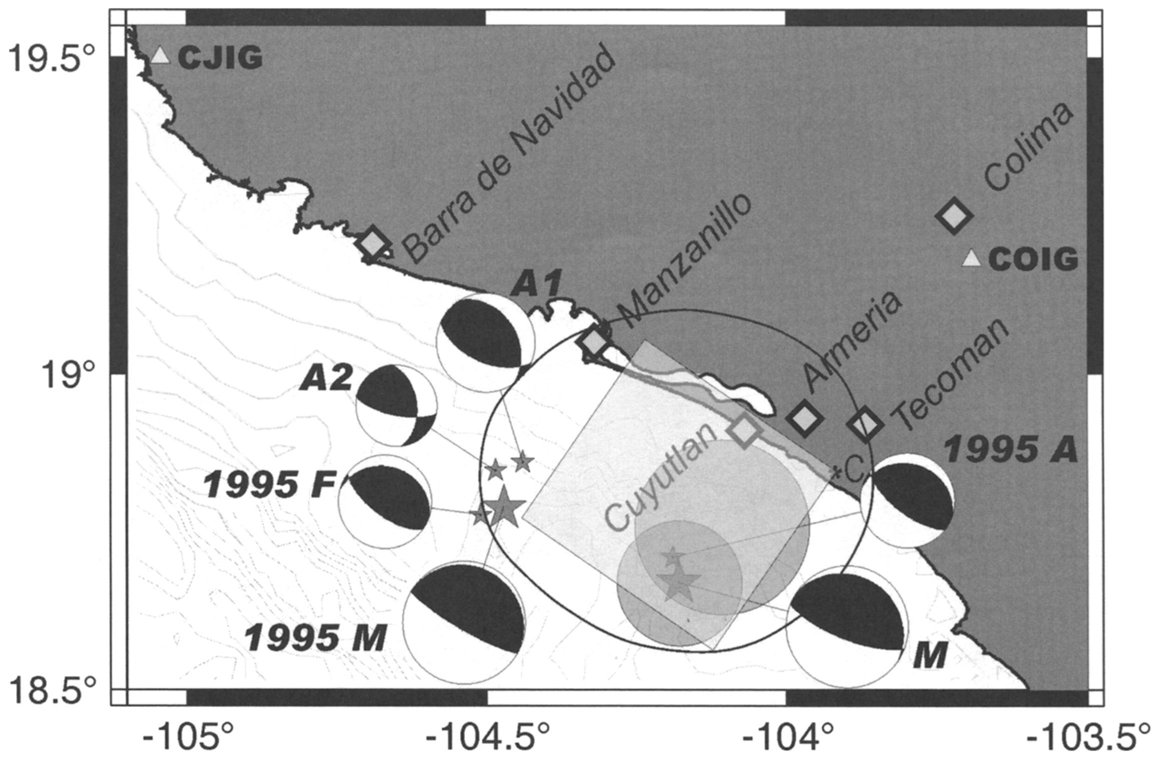

▲ **Figure 2.** Locations and focal mechanisms of the Tecomán mainshock (*M*) and two of its largest aftershocks (*A*1, *A*2). Foreshock, mainshock, and aftershock epicenters of the 9 October 1995 (M_w 8.0) earthquake are denoted by 1995F, 1995M, and 1995A, respectively. The contour shows the aftershock area of the Tecomán earthquake estimated from RESCO locations (four days of activity, ~120 events). The circles indicate the rupture areas of two subevents (see text). The rectangular fault with an average slip of 200 cm fits the static horizontal permanent deformation in Manzanillo (see text).

At farther distances the earthquake was recorded in the free field by the BB stations operated by SSN, by elements of the Guerrero Accelerograph Array (GAA), and by some stations operated by Centro Nacional de Prevención de Desastres (CENAPRED) and CIRES. The event was also recorded by two microarrays in the Valley of Mexico and by accelerographs installed in buildings in Mexico City and Acapulco. Table 2 lists A_{max} values at free-field, hard sites that were available at the time of writing this report. Figure 3 shows the locations of these stations.

A tsunami was recorded by a tide gauge in Manzanillo. The peak-to-peak amplitude of the tsunami was ~1 m, roughly about half of the peak amplitude recorded during the 1995 earthquake. A permanent GPS receiver in Manzanillo reveals a static deformation of 8.0 cm to the south and 2.5 cm to the west. It is difficult to estimate the vertical deformation because of large scatter in the data.

TABLE 2
Peak Accelerations on Hard Sites during Tecomán Earthquake

Station Code	Hypocentral Distance (km)	A_{max} (gal)		
		NS	EW	Z
COIG[1]	80	>47.8[4]	>70.5[4]	>72.1[4]
CJIG[1]	138	38.8	16.2	15.9
CALE[2]	159	28.1	27.8	14.7
VILE[2]	216	10.4	11.1	6.8
UNIO[2]	256	12.3	8.2	8.9
ZIIG[1]	312	5.4	5.4	3.7
PET2[2]	333	3.7	3.6	3.7
COYQ[2]	353	4.9	3.4	3.7
CAIG[1]	453	1.4	1.5	1.2
ZAIG[1]	486	1.6	2.0	2.6
PLIG[1]	489	7.8	3.4	4.0
ACAJ[3]	498	2.0	1.5	1.3
CUER[3]	520	6.9	8.2	4.6
CNPJ[3]	537	4.6	4.3	2.7
CUIG[1]	537	4.2	4.2	2.0
YAIG[1]	544	3.2	2.2	2.1
ESTS[3]	545	2.0	2.0	1.3
MAIG[1]	560	0.65	0.41	0.39
TPIG[1]	723	4.2	2.3	3.0
PNIG[1]	783	0.99	0.41	0.97
OXIG[1]	810	3.6	2.3	2.0
CMIG[1]	1002	1.2	0.42	0.62
CCIG[1]	1307	0.64	0.37	0.44

1. Station operated by SSN.
2. GAA station operated by Instituto de Ingeniería, UNAM and University of Nevada, Reno.
3. Station operated by CENAPRED.
4. Peak value during *P*-wave group, hence a lower bound.

Gross Source Characteristics as Inferred from COIG Records

Although only about 10 sec of the accelerogram is available at COIG, it provides useful information with which we can investigate the source characteristics of the earthquake. COIG is located close to the city of Colima (Figure 2). Thus, an analysis of the recording from this station may help us understand the damage pattern left by the earthquake in the city.

With respect to the RESCO location, COIG lies at an epicentral distance of 77 km at an azimuth of N37°E (Figures 1 and 2). The acceleration and velocity time histories at COIG are shown in Figures 4 and 5, respectively. A faint *P*-wave arrival is visible in the accelerograms after about 0.5 sec. We assume that this arrival comes from the RESCO epicenter. The velocity traces demonstrate that the earthquake began with a small event and, progressively, cascaded into larger subevents. A negative ramp with small slope is visible until 5.4 sec after the arrival of the first *P* wave, followed by a sudden increase in the slope (Figure 5). We interpret this change in the slope to represent the rupture of a large subevent. To estimate the azimuth, ϕ_s, of COIG with respect to this subevent, we rotated the north-south and east-west velocity seismograms into radial (R) and transverse (T) components, varying ϕ_s. The minimum amplitude on the T component was found for $\phi_s = 38°$ (Figure 5). Recall that ϕ_s of COIG from the RESCO epicenter is N37°E. This suggests that the rupture (at least during the first 10 sec or so of the COIG record) propagated toward COIG and the city of Colima.

We modeled the R and Z velocity traces in Figure 5 using two subevents. The far-field *P*-wave synthetics were computed using the circular fault model of Sato and Hirasawa (1973). For the first subevent, station COIG is located at a hypocentral distance R of 80 km from the center of the rupture area, with $\theta = 60°$, $\varphi = 180°$. We assume a *P*-wave speed, α, of 6.8 km/s and a Poisson solid. The free-surface effect is roughly approximated by multiplying the synthetics by a factor of 2. The angle of incidence at the half space, i_0, is taken as 75° from vertical. The first subevent is well fit with $M_0 = 3.0 \times 10^{26}$ dyne, stress drop $\Delta\sigma$ = 125 bars, and a rupture speed $V_R = 0.5\beta$, where β is the shear-wave speed (Figure 5).

The location of the second, large subevent can be estimated from $V_R = 0.5\beta$ and the time difference of 5.4 sec at COIG between the arrivals of *P* waves from the two subevents. The location of the second subevent is 15 km from the epicenter toward COIG. To estimate the source characteristics of the second subevent we followed the same procedure as before. The new set of parameters is $R = 67$ km, $\theta = 53°$, $\varphi = 180°$, $i_0 = 63°$. The synthetics fit the observed velocities with $M_0 = 1.3 \times 10^{27}$ dyne (M_w 7.3), assuming $\Delta\sigma = 125$ bars and $V_R = 0.9\beta$ (Figure 5). The radius, a, and the average slip, Δu, for each of the subevents can be estimated from the relations (Keilis-Borok, 1959)

$$\Delta\sigma = \left(\frac{7\pi}{16}\right)\mu\left(\frac{\Delta u}{a}\right) = \left(\frac{7}{16}\right)\left(\frac{M_0}{a^3}\right).$$

This yields:

First subevent: a =10.2 km and Δu=231 cm.
Second subevent: a=16.6 km and Δu=380 cm.

Figure 2 shows the locations and sizes of the two circular rupture areas.

The permanent horizontal deformation at Manzanillo (8.0 cm to the south and 2.5 cm to the west) can be explained by a rectangular fault (shown in Figure 2) with the following parameters: length = width = 40 km, average dislocation 200 cm, azimuth of the fault 305°, dip 17°, rake 90°, depth

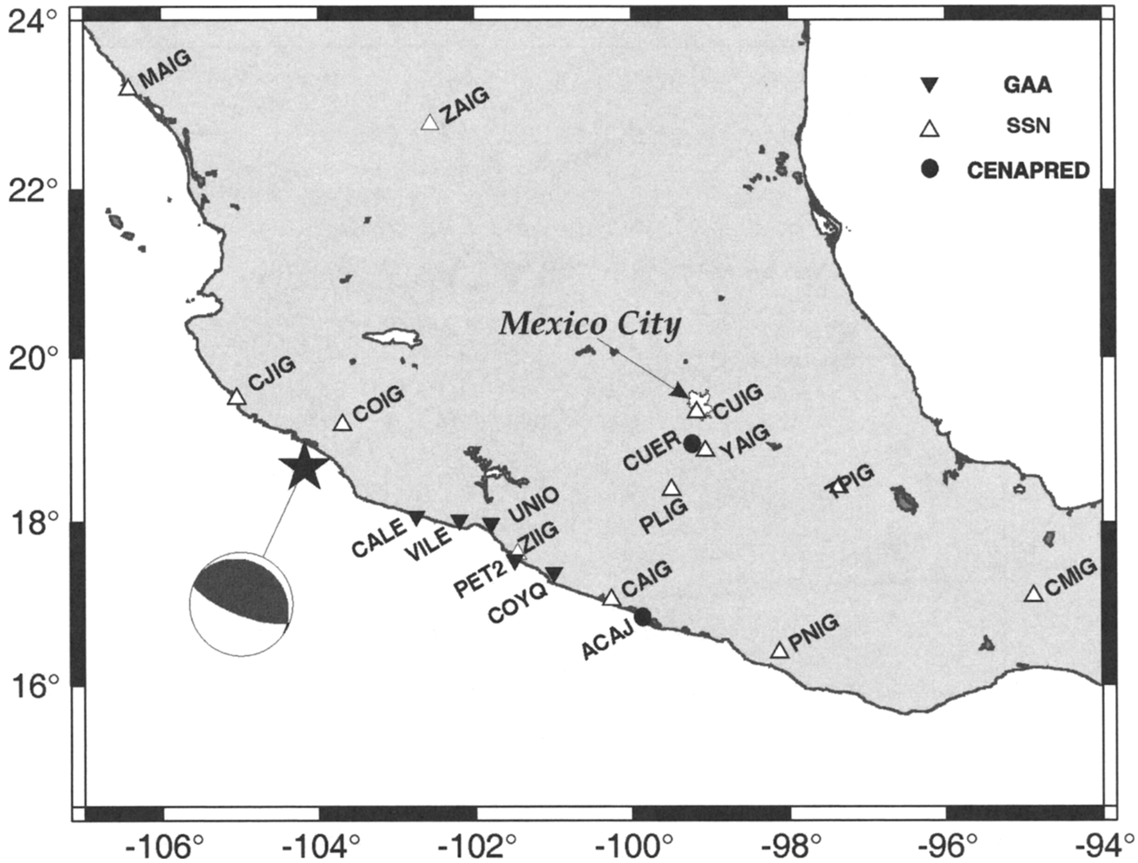

▲ **Figure 3.** Locations of free-field, hard sites where strong motions from the Tecomán earthquake were recorded.

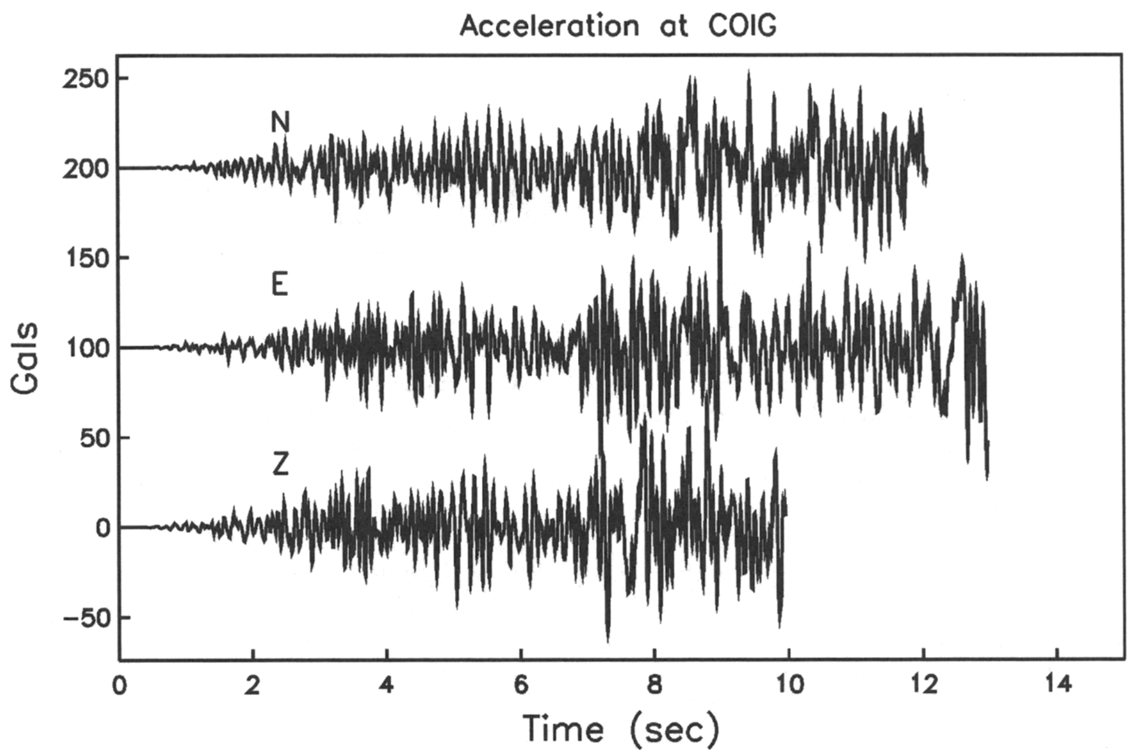

▲ **Figure 4.** Accelerogram of the mainshock at COIG, a BB station near the city of Colima. The station failed after recording ~10 sec of signal, essentially the *P*-wave group. A_{max} on north-south, east-west, and Z components are 48, 71, and 72 gals, respectively.

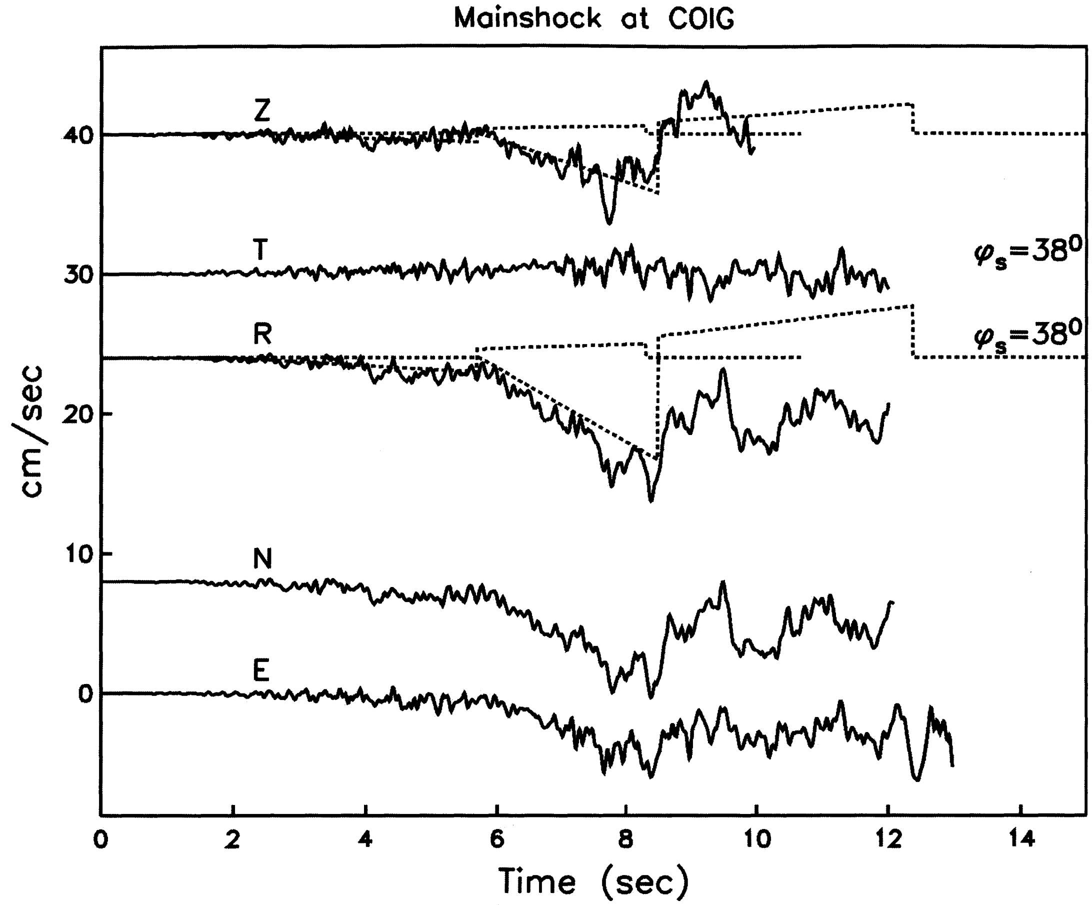

▲ **Figure 5.** Velocity seismograms of *P*-wave group at COIG (obtained by direct integration of the accelerograms shown in Figure 4). Note a negative ramp in the north-south, east-west, and *Z* traces with a small slope that is followed by another with a larger slope. We identify the two slopes with two subevents. *R* and *T* indicate transverse and radial components resulting from a N38°E rotation of north-south and east-west components. This rotation gives minimum *T* amplitude, suggesting that COIG is situated N38°E with respect to the large subevent that begins at 5.4 sec. Dashed lines are synthetics corresponding to two circular sources (see text).

of point C = 30 km. The computations were made using Okada's (1975) analytical expressions.

Yagi (2003) has mapped the rupture evolution, the source-time function, and the slip distribution on the fault by inverting broadband, teleseismic *P* waves. His preliminary results show a unilateral rupture toward the northwest of about 40 km, with maximum dislocation of 300 cm occurring 15 km northwest of the epicenter. The moment release is small in the first 3 sec. The major part of the moment release occurs between 3 and 15 sec after the initiation of the rupture, with some slow slip extending till about 27 sec. Yagi's results roughly agree with the gross source characteristics as seen from COIG data. In both cases, the rupture propagates down dip and rupture initiates with small subevents.

The peak horizontal acceleration, A_{max}, at COIG during the *P* wave on the north-south component was 70 gals. Assuming the *S*-wave A_{max} value to be two or more times the corresponding value during the *P* wave, we expect A_{max} of 140 gals or more at the hard-rock site of COIG. A_{max} at soil sites in the nearby city of Colima is, then, expected to have been larger than this value.

Attenuation of Strong Ground Motion

Figure 6 illustrates A_{max} values on the two horizontal components as a function of hypocentral distance *R*. Only the recordings obtained on hard-rock sites are included in the figure. Since even "hard" sites in the Valley of Mexico are known to suffer amplification of seismic waves (Singh *et al.*, 1995), these sites are excluded from the plot. For comparison, Figure 6 includes the corresponding data from the Copala earthquake of 14 September 1995, which was also M_w 7.4. Superimposed on these plots is the predicted A_{max} curve for a M_w 7.4 earthquake computed using the regression relation of Ordaz *et al.* (1989). The data from inland and coastal sites are plotted by different symbols. For the Copala earthquake, the predicted values are close to observed ones, although there is a hint that the observed values at inland sites are a little higher than those at coastal ones. For the Tecomán earthquake, the predicted values are consistently lower than the observed ones. This suggests that the Tecomán earthquake was more energetic at higher frequencies than an "average" event. At larger distances (400 < *R* < 1,400 km), the observed values at inland sites are much higher than the corresponding values at

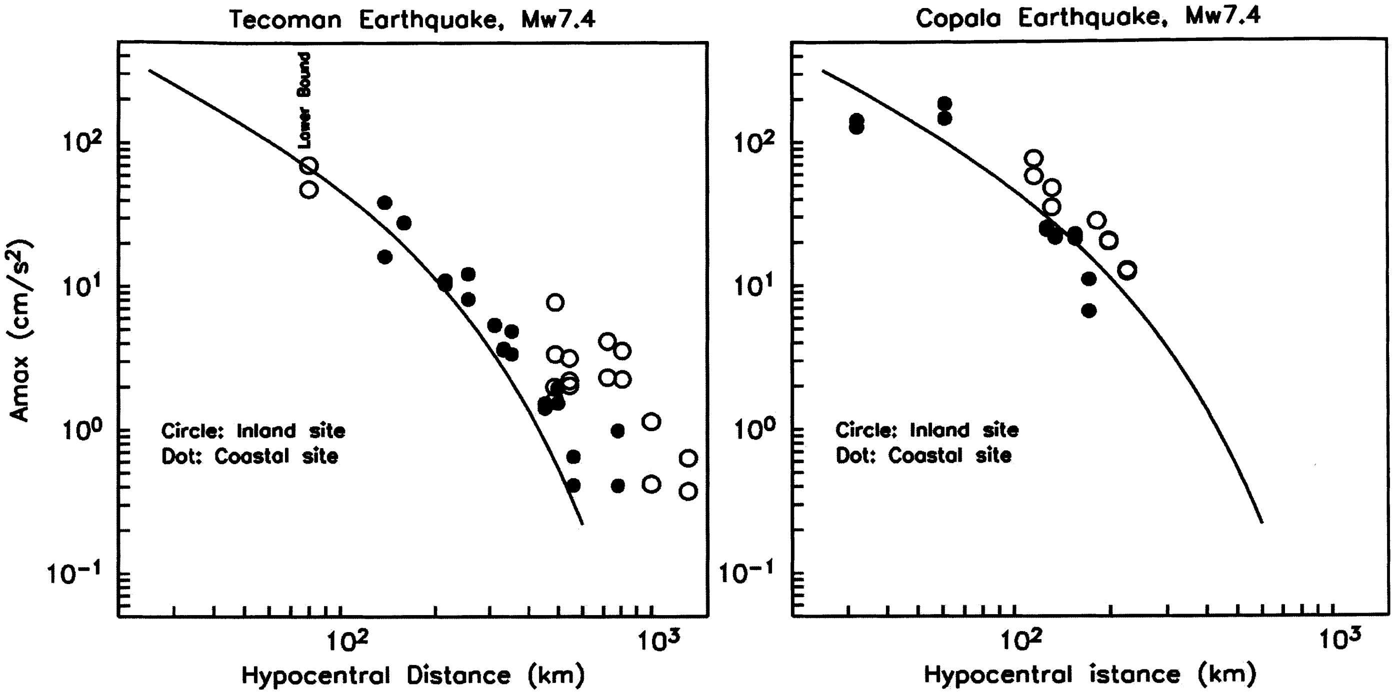

▲ **Figure 6.** Horizontal peak acceleration, A_{max}, as a function of hypocentral distance *R* at free-field, hard sites. Left: Tecomán earthquake. Right: Copala earthquake. Open circle: inland site; solid circle: coastal site. Dashed line: predicted curve for M_w7.4 (Ordaz *et al.*, 1989).

TABLE 3
Source Parameters of the Two Largest Aftershocks of the Tecomán Earthquake

Date	H:M:S	Source	Lat	Long	Depth (km)	Magnitude	M_0 (dyne-cm)	Strike	Dip	Rake
22 Jan 2003	19:41:42	SSN	18.76°	–104.54°	14	M_e5.7, M_w5.7	3.4×10^{24}	304°	38°	84°
	19:41:52	CMT	18.96°	–104.47°	15	M_w6.2	2.3×10^{25}	328°	38°	118°
22 Jan 2003	20:15:38	SSN	18.85°	–104.49°	5	M_e5.1, M_w5.3	4.7×10^{23}	353°	48°	153°

coastal sites. An examination of the recordings suggests that the cause of this difference is the dispersed character of the waves propagating along the coast as compared to the pulse-like character of the wave traveling inland.

In Figure 6 the predicted curve at large distances underestimates the observed ones by more than an order of magnitude. This large discrepancy reflects lack of data at distances > 300 km at the time the regression analysis was performed.

Aftershocks

Large/great Mexican earthquakes in general, and those in Jalisco, Colima, and Michoacán in particular, are known to produce relatively small number of aftershocks (Singh and Suárez, 1988). The Tecomán earthquake was no exception. Only two aftershocks exceeding $M_w \geq 5$ occurred during the first month following the mainshock. Table 3 lists their source parameters and Figure 2 illustrates their locations. It is interesting to note that these two aftershocks occurred near the foreshock (6 October 1995, M_w 5.8) of the 1995 event, and the rupture of the Tecomán earthquake commenced near the largest aftershock (12 October 1995, M_w 5.9) of the 1995 earthquake (Figure 2).

DAMAGE FROM THE EARTHQUAKE

The Tecomán earthquake produced moderate to high intensities near the epicentral region. Damage was concentrated along a wide strip extending from the coastal region, near the epicentral area, toward the north. Compared to the city of Colima, the damage was less severe in Manzanillo and Cihuatlán. The most heavily damaged villages were located in the state of Colima and in 25 municipalities of the neighboring states of Jalisco and Michoacán. According to civil protection officials, the earthquake left 21 persons dead.

Landslides were observed near the epicentral region and the city of Colima. Liquefaction was reported along the coast but was smaller than expected for this magnitude event. In Villa de Álvarez, a residential area northwest of Colima, large settlements and openings in the ground were visible.

A few bridges along the coast and inland suffered damage. In some cases, seismic stops at the ends of bent caps exhibited moderate to severe shear damage. In other bridges, settlement of abutments was observed.

According to the Mexican National Water Commission, the Trojes and Las Piedras embankment dams, both filled at the operation levels of the reservoirs and located about 175 km from the epicenter, were damaged. Measurable deformation occurred on both dams, including settlement, lateral spreading, and, as a result, longitudinal cracking. The deformation patterns and the type of cracking were associated with compaction and shear distortion (lateral spreading) on the embankments under dynamic shaking.

The Manzanillo thermal power plant suffered damage in the water intake structure and at the substation. As mentioned earlier, a peak horizontal acceleration of 323 gals was recorded at this site in the free field.

Structural damage primarily affected housing. About 15,000 houses were reported damaged, roughly 3,000 of them severely. The most significant damage was observed in adobe and unreinforced brick masonry houses. Damage typically included wall-inclined cracking, vertical cracking at wall intersections, and roof failure, particularly in adobe houses. It was also apparent that corner houses suffered more damage. This is credited to the lack of confinement from adjoining structures, to the presence of openings on the façade walls, and perhaps to torsional demands.

Confined masonry is the most popular reinforced masonry construction style in the region. This system consists of reinforced vertical and horizontal concrete elements that are intended to confine the load-bearing masonry walls and to tie them to the floor and roof. When properly designed and constructed, such masonry houses exhibited adequate performance. The vulnerability of this construction style was apparent when tie-columns were small or scarce in number, especially at the edges of door openings. From the overall level of damage recorded in the city of Colima, the ground accelerations may have been 0.1 to 0.15 g, somewhat less than the estimation above based on the COIG record.

Compared to nonengineered buildings, damage in engineered constructions, either of steel, reinforced concrete, or masonry, was not as extensive. Several dozen schools were reported with light to moderate damage; some of these had been slightly damaged during the 9 October 1995 earthquake (M_w 8.0) but had not been repaired.

Few cases of damage in historical monuments were reported. The church of Coquimatlán lost the upper part of the bell tower. Some monuments that had been damaged in previous earthquakes and subsequently repaired and strengthened performed well, suggesting that the rehabilitation techniques were satisfactory.

Observed A_{max} values in the lakebed zone of Mexico City were between 20 to 30 gals (2 to 5 gals in the hill zone). Although no damage was reported in the city, there was general panic in the population. Many people in the city still vividly remember the devastating consequences of the 19 and 21 September 1985 earthquakes (M_w 8.0, 7.6).

ISOSEISMAL MAP

Based on reports from local government authorities, telephone inquiries with civil protection agencies, newspaper accounts, and reports from field inspection teams, an isoseismal map of the earthquake was constructed (Table 4, Figure 7). The region of highest modified Mercalli intensity (MMI), VIII, includes Tecomán, Armería, and the city of Colima. Contours of MMI VII and VIII are elongated in the north-south direction, perhaps reflecting source directivity as discussed above. The MMI was lower in Manzanillo and higher in the city of Colima during the Tecomán earthquake than during the 1995 earthquake.

In Table 5 we summarize intensities in Manzanillo and the city of Colima during large/great earthquakes since 1900. We note that MM intensities greater than or equal to VII have occurred six and seven times in Manzanillo and the city of Colima, respectively, in roughly the last 100 years.

DISCUSSION AND CONCLUSION

It has been suggested that the subducted part of the RIVE-COCOS plate boundary is located below, and is parallel, to the Southern Colima Rift (Figure 1). Since the hypocenters of the aftershocks of the Tecomán earthquake lie below the rift, this suggests that the rupture area of the event extended over both subducted oceanic plates. The aftershock zone is nearly circular in shape with a radius of about 30 km. This area of the plate interface was left unbroken during the 1932 events (M_s 8.2, 7.8) and the 1973 earthquake (M_w 7.6). Some of this area, however, overlaps with the southeast end of the aftershock zone of the 1995 earthquake (M_w 8.0). In fact, the foreshock (M_w 5.8) and the largest aftershock (M_w 5.9) of the 1995 earthquake were located in the aftershock area of the Tecomán event.

The recordings, especially the 10 sec of *P*-wave accelerogram at COIG, a broadband station near the city of Colima, show that the earthquake initiated with a small subevent and cascaded in larger subevents, with a directivity toward N38°. This directivity may have been the cause of larger damage in the city of Colima than in Manzanillo. The peak horizontal acceleration at COIG during the *P*-wave group of 72 gals provides a lower bound for A_{max} in the city of Colima; at hard-rock sites the A_{max} may have been two or more times greater than this value. The observed A_{max} versus hypocentral distance, *R*, data is well above the predicted curve from a regression relation, especially at inland stations. This discrepancy has been observed before for Mexican subduction earthquakes recorded at distances greater than 400 km. This discrepancy is a consequence of lack of data at farther distances when the regression relation was derived. There is clearly a need for a new regression study.

The damage was extensive in the entire state of Colima and in some of the municipalities of the adjoining states of Jalisco and Michoacán. About 15,000 dwellings were damaged, a fifth of them badly. Landslides occurred near the epi-

TABLE 4 MM Intensities during the Tecomán Earthquake		
State	**City/Town/Municipality**	**MMI**
Aguascalientes	Aguascalientes	IV–V
Colima	Armería	VIII
Colima	Colima	VIII
Colima	Coquimatlán	VIII
Colima	Ixtlahuacán	VIII
Colima	Manzanillo	VII–VIII
Colima	Minatitlán	VIII
Colima	Tecomán	VIII
Colima	Villa de Álvarez	VIII
Distrito Federal	Álvaro Obregón	IV–V
Distrito Federal	Azcapotzalco	V
Distrito Federal	Benito Juárez	V
Distrito Federal	Coyoacán	IV–V
Distrito Federal	Cuajimalpa	V
Distrito Federal	Gustavo A. Madero	V
Distrito Federal	Iztacalco	V
Distrito Federal	Xochimilco	V
Distrito Federal	Iztapalapa	V
Distrito Federal	Gustavo A. Madero	V
Distrito Federal	Venustiano Carranza	V
Durango	Durango	II
Estado de México	Toluca	IV
Guanajuato	Guanajuato	IV
Guanajuato	Irapuato	V
Guanajuato	Celaya	IV
Guanajuato	León	IV–V
Guanajuato	Salamanca	IV
Guerrero	Acapulco	III–IV
Guerrero	Chilpancingo	IV
Hidalgo	Pachuca	II–III
Jalisco	Ameca	VI
Jalisco	Autlán	VII
Jalisco	Cihuatlán	VII
Jalisco	Ciudad Guzmán	VI–VII
Jalisco	Chapala	V
Jalisco	Cocula	VI
Jalisco	Cuautitlán	VII
Jalisco	Guadalajara	V–VI
Jalisco	Gómez Farías	VI–VII
Jalisco	Jocotepec	VI
Jalisco	Mazamitla	V–VI
Jalisco	Pihuamo	VII

TABLE 4 (Continued) MM Intensities during the Tecomán Earthquake		
State	**City/Town/Municipality**	**MMI**
Jalisco	Puerto Vallarta	V–VI
Jalisco	Cabo Corrientes	VI
Jalisco	Tomatlán	VI
Jalisco	El Salto	V
Jalisco	Zapotitlán de Vadillo	VII–VIII
Jalisco	Tequila	V
Jalisco	Tolimán	VII
Jalisco	Tuxpan	VII
Jalisco	Zapopan	V
Jalisco	Zapotiltic	VI–VII
Michoacán	Apatzingan	V
Michoacán	Ciudad Hidalgo	IV
Michoacán	Chinicuila	IV
Michoacán	Coahuayana	VIII
Michoacán	Coalcomán	VII
Michoacán	Cotija	V
Michoacán	Morelia	V
Michoacán	Pamatácuaro	V
Michoacán	Purépero	V
Michoacán	Uruapan	V
Michoacán	San Juan Nuevo	V
Michoacán	Tangamandapio	V
Michoacán	Zamora	V
Morelos	E. Zapata	IV
Morelos	Yautepec	III–IV
Morelos	Yecapixtla	III–IV
Morelos	Panchimalco	IV
Nayarit	Tepic	V
Nayarit	San Blas	IV–V
Nayarit	Santiago Ixcuintla	IV
Puebla	Puebla	II–III
Querétaro	Querétaro	III
Sinaloa	Mazatlán	II–III
Tlaxcala	Tlaxcala	II–III
San Luis Potosí	Mexquitic	III
San Luis Potosí	San Luis Potosí	III–IV
Veracruz	Veracruz	II
Veracruz	Jalapa	II
Veracruz	Córdoba	III
Veracruz	Orizaba	III
Zacatecas	Zacatecas	II

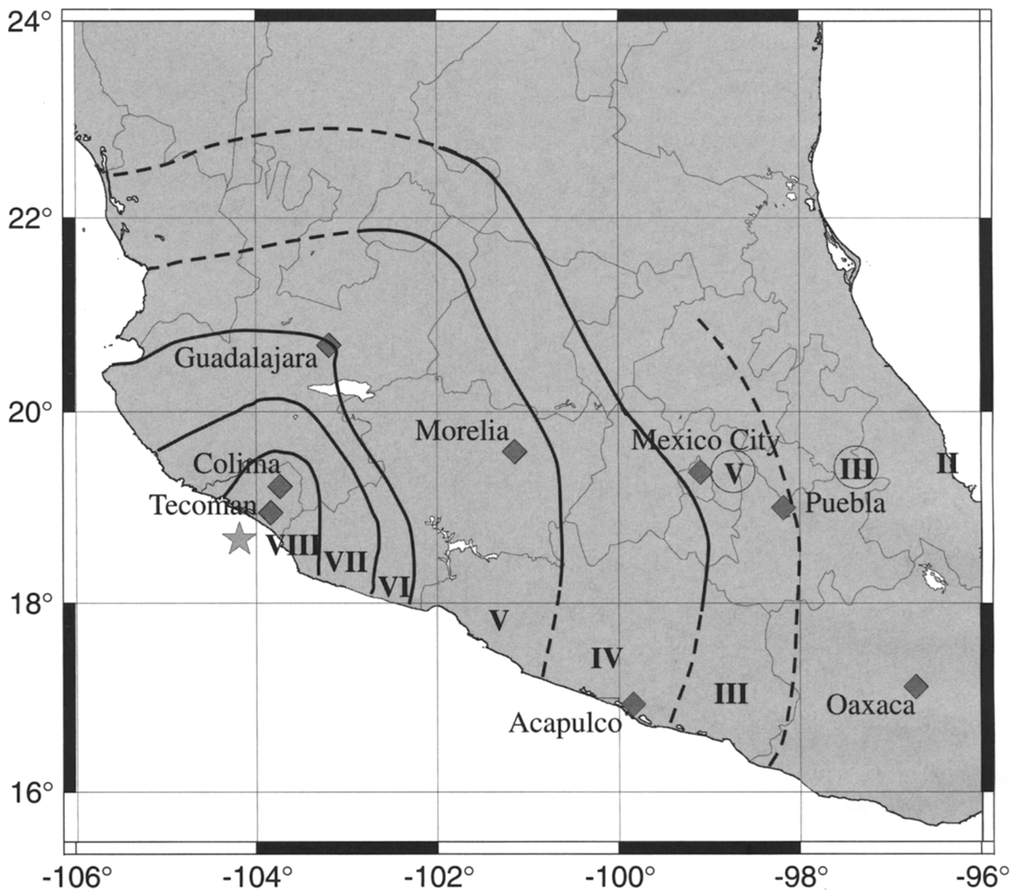

▲ **Figure 7.** Isoseismal map (modified Mercalli intensities) of the Tecomán earthquake. North-south elongation of MM intensity VIII may be due to source directivity.

TABLE 5
MM Intensities of VII or Greater in Manzanillo and Colima since 1900

Date	Magnitude	Manzanillo	City of Colima
20 January 1900	M 7.4	—	VIII
3 June 1932	M_S 8.2	VIII	VIII
18 June 1932	M_S 7.8	VIII–IX	IX
15 April 1941	M_S 7.6	VIII	X
30 January 1973	M_w 7.6	VIII	VIII
8 October 1995	M_w 8.0	VIII–IX	VII
22 January 2003	M_w 7.4	VII–VIII	VIII

central region and the city of Colima. Liquefaction was reported along the coast. On the positive side, very few cases of structural damage were recorded in engineered buildings, either of steel or reinforced concrete.

A simultaneous inversion of local/regional and teleseismic data is needed to map the rupture history and the directivity of the source better. The azimuthal variation of source-time function, retrieved from deconvolution of the mainshock recordings by aftershock recordings, may also reveal the directivity. Several groups recorded the aftershocks of the earthquake by deploying portable digital seismographs in the field. These data should lead to several interesting studies, including a better map of the aftershock zone and the geometry of the Wadati-Benioff zone.

Some of the mainshock data, reported in this study, are available for distribution. Please contact the senior author who, in turn, will redirect the request to the group in charge of the data.

ACKNOWLEDGMENTS

We thank William Bandy for discussions regarding the tectonics of the region and J. M. Espinosa for providing us with paper copies of the Manzanillo accelerograms. Kristine Larson provided us with permanent deformation data at Manzanillo. We are grateful to Susan Hough for her thoughtful comments and revision of the manuscript. The research was partly supported by DGAPA, UNAM project IN111601, and CONACYT projects R32346-T and 36671-T. It was also supported in part by The National Science Foundation under Grant Number 00000050.

REFERENCES

Bandy, W., C. Mortera, J. Urrutia, and T. W. C. Hilde (1995). The subducted Rivera-Cocos Plate boundary: Where is it, what is it, and what is its relationship to the Colima rift?, *Geophysical Research Letters* **22**, 3,075–3,078.

Bernal Carrera, Z. R. (2000). *Posibles escenarios de rupturas durante el sismo de Jalisco del 9 de octubre de 1995 (Mw=8.0) y sus implicaciones*, M.S. thesis, Dirección General de Posgrado en Ciencias de la Tierra, Instituto de Geofísica, UNAM.

Courboulex, F., S. K. Singh, J. F. Pacheco, and C. J. Ammon (1997). The 1995 Colima-Jalisco, Mexico earthquake (Mw 8): A study of the rupture process, *Geophysical Research Letters* **24**, 1,019–1,022.

Keilis-Borok, V. (1959). On estimation of the displacement in an earthquake source and of source dimensions, *Annali di Geofisica (Rome)* **12**, 205–214.

Kostoglodov, V. and W. Bandy (1995). Seismotectonics constraints on the convergence rate between the Rivera and North American Plates, *Journal of Geophysical Research* **100**, 17,977–17,989.

Melbourne, T., I. Carmichael, C. DeMets, K. Hudnut, O. Sánchez, J. Stock, G. Suárez, and F. Webb (1997). The geodetic signature of the M8.0 Oct. 9, 1995, Jalisco subduction earthquake, *Geophysical Research Letters* **24**, 715–718.

Ordaz, M., J. M. Jara, and S. K. Singh (1989). Riesgo sísmico y espectros de diseño en el estado de Guerrero, *Mem. VIII Congreso Nacional de Ingeniería Sísmica*, Vol. II, D40–D56, Acapulco.

Ortiz, M., S. K. Singh, J. Pacheco, and V. Kostoglodov (1998). Rupture length of the October 9, 1995 Colima-Jalisco (Mw 8) estimated from tsunami data, *Geophysical Research Letters* **25**, 2,857–2,860.

Ortiz, M., J. González, J. Reyes, C. Nava, E. Torres, G. Sáens, and J. Arrieta (1996). *Efectos costeros del tsunami del 9 de octubre en la costa de Colima y Jalisco*, Technical Report, CICESE, Ensenada, Baja California.

Pacheco, J., S. K. Singh, J. Domínguez, A. Hurtado, L. Quintanar, Z. Jiménez, J. Yamamoto, C. Gutiérrez, M. Santoyo, W. Bandy, M. Guzmán, V. Kostoglodov, G. Reyes, and C. Ramírez (1997). The October 9, 1995 Colima-Jalisco, Mexico earthquake (M_W 8): An aftershock study and a comparison of this earthquake with those of 1932, *Geophysical Research Letters* **24**, 2,223–2,226.

Okada, Y. (1985). Surface deformation due to shear and tensile faults in a half space, *Bulletin of the Seismological Society of America* **75**, 1,135–1,154.

Reyes, A., J. N. Brune, and C. Lomnitz (1979). Source mechanism and aftershock study of the Colima, Mexico earthquake of January 30, 1973, *Bulletin of the Seismological Society of America* **69**, 1,819–1,840.

Sato, T. and T. Hirasawa (1973). Body wave spectra from propagating shear cracks, *Journal of Physics of the Earth* **21**, 415–431.

Shapiro, N. M., S. K. Singh, and J. Pacheco (1998). A fast and simple diagnostic method for identifying tsunamigenic earthquakes, *Geophysical Research Letters* **25**, 3,911–3,914.

Singh, S. K., L. Ponce, and S. P. Nishenko (1985). The great Jalisco, Mexico, earthquakes of 1932: Subduction of the Rivera Plate, *Bulletin of the Seismological Society of America* **75**, 1,301–1,313.

Singh, S. K. and G. Suárez (1988). Regional variation in the number of aftershocks ($mb \geq 5$) of large subduction zone earthquake ($Mw \geq 7$), *Bulletin of the Seismological Society of America* **78**, 230–244.

Singh, S. K., R. Quaas, M. Ordaz, F. Mooser, D. Almora, M. Torres, and R. Vasquez (1995). Is there truly a "hard" rock site in the Valley of Mexico?, *Geophysical Research Letters* **22**, 481–484.

Yagi, Y. (2003). Preliminary results of rupture process for January 22, 2003 Colima, Mexico, earthquake, http://iisee.kenken.go.jp/staff/yagi/eq/colima/colima.html.

UNAM
Instituto de Geofísica
C.U. 04150 México D.F.
México
krishna@ollin.igeofcu.unam.mx
(S.K.S.)